Article
Journal of Nanoscience and Nanotechnology
Vol. 15, 244–247, 2015
www.aspbs.com/jnn

Efficiencies of Dye-Sensitized Solar Cells with Hollow SnO_2 Nanofiber/TiO_2 Nanoparticle Composite Photoanodes

Ji-Hye Lee[1], Kyun Ahn[2], Soo-Hyung Kim[2], Se-Young Jeong[2], Jong-Sung Bae[3], Tae-Eun Hong[3], Hyun-Gyu Kim[3], and Chae-Ryong Cho[1, 2, *]

[1] *Department of Applied Nanoscience, Pusan National University, Busan 609-735, Korea*
[2] *Department of Nano Fusion Technology and College of Nanoscience and Nanotechnology, Pusan National University, Busan 609-735, Korea*
[3] *Busan Center, Korea Basic Science Institute, Busan 618-230, Korea*

In this study, we present dye-sensitized solar cells (DSSCs) with improved efficiencies by using SnO_2/TiO_2 composite photoanodes containing SnO_2 at various concentrations. The composites consisted of hollow nanofibers (*h*-NFs) of SnO_2 and TiO_2 nanoparticles (NPs). The combination of the large surface area of the NPs and the efficient charge transport in the *h*-NFs make the use of the SnO_2/TiO_2 composites advantageous. DSSCs in which composite photoanodes with 50 wt% *h*-NFs were incorporated showed enhanced efficiencies that were 20% higher than the efficiencies of cells containing TiO_2 NP-based photoanodes. These results indicated the improved electron diffusion length and shorter electron transfer time in the composite structures due to the crosslinking between *h*-NFs and NPs.

Keywords: Hollow SnO_2 Nanofiber, Composite Photoanode, Dye-Sensitized Solar Cell.

1. INTRODUCTION

Dye-sensitized solar cells (DSSCs) have attracted much interest in the past decade as promising cost-effective next-generation photovoltaic solar cells.[1–3] Conventional DSSCs based on mesoporous TiO_2 nanoparticles (NPs), which possess high surface areas, have been widely used as photoanodes.[4] However, a major drawback of applying TiO_2 NP-based photoanodes in DSSCs is the inefficient electron transport due to grain boundary scattering between NPs. To reduce grain boundary scattering, considerable efforts have been devoted to the development of one-dimensional (1D) nanostructures.[5, 6] These 1D nanostructures can provide efficient pathways for electron transport and reduce charge recombination due to the presence of fewer grain boundaries. To improve the performance of NP-based DSSCs, it have been studied on the 1D nanostructure and NPs composite photoanode, which provides large surface areas of NPs for dye adsorption and a fast electron transport of 1D nanostructure.[6, 7] However, there have been no reports on the TiO_2 NPs/SnO_2 hollow nanofibers (*h*-NFs) composite-based DSSCs.

In this paper, we used the composites of TiO_2 NPs and *h*-NFs of SnO_2, which has higher electron mobility ($\sim$100 to 200 $cm^2/V \cdot s$) than TiO_2, as photoanodes to fabricate DSSCs. We investigated the effect of the ratio of NPs to *h*-NFs on the performance of the DSSCs.

2. EXPERIMENTAL DETAILS

The SnO_2 *h*-NFs were fabricated by electrospinning as previously reported.[6] Five different pastes containing a mixture of SnO_2 *h*-NFs and TiO_2 NPs were prepared with the concentration of the SnO_2 *h*-NFs fixed at 0, 25, 50, 75 and 100 wt%. The pastes were then printed on F-doped SnO_2 (FTO)/glass substrates and annealed at 500 °C for 2 h. The specific surface areas of SnO_2 *h*-NFs samples were not higher than NPs used in this experiment. DSSCs with an area of 5×5 mm^2 and thickness of 20 μm were fabricated by using N719 dye (Solaronix), Iodolyte AG-50 electrolyte (Solaronix), and Pt/FTO/glass as the counter electrode.

*Author to whom correspondence should be addressed.

1533-4880/2015/15/244/004 doi:10.1166/jnn.2015.8399

The structures and surface morphologies of these samples were examined by X-ray diffraction (XRD) [Phillips, X'pert Pro] in the θ–2θ scan mode with 2θ ranging from 20° to 80° using Cu-$K_{\alpha 1}$ (wavelength $\lambda = 1.5406$ Å) as the incident X-ray beam and by field emission scanning electron microscopy (FESEM) [Hitachi, S-4700] at an operating voltage of 15 kV, respectively. The current density–voltage (J–V) characteristics of the DSSCs were measured under AM 1.5 simulated illumination with an intensity of 100 mW/cm^2 [PEC-L11 model, Pecell Technologies Inc.]. The intensity of illumination in terms of sunlight was calibrated using a standard Si photodiode detector with a KG-5 filter. Electrochemical impedance spectroscopy (EIS) was carried out in the frequency range 0.01–100 kHz at an open-circuit voltage using a potential pulse with amplitude of 10 mV.

3. RESULTS AND DISCUSSION

Figure 1 shows FESEM image of the SnO_2 h-NFs and that of the SnO_2 h-NF/TiO_2 NP composite film containing 50 wt% SnO_2 h-NFs. Figure 1(a) is the image of ground SnO_2 h-NFs used to prepare the paste for the fabrication of DSSC photoanodes. The total diameter of the SnO_2 h-NFs was about 500 nm and the thicknesses of the inner hollow and the shell were about 400 nm and 50 nm, respectively. The SnO_2 h-NFs, composed of large grains, were uniform in shape and consisted of smooth surfaces. Figure 1(b) shows the surface and cross section images of the composite film. The composite films were compact and the SnO_2 h-NFs were distributed uniformly among the NPs, as shown in SEM images of Figure 1(b). In addition, the morphology of the h-NFs was also maintained. The thickness of the composite film was about 20 μm, as shown in the inset of Figure 1(b).

Figure 2 shows the XRD patterns of the composite films with different concentrations of SnO_2 h-NFs. In samples with 0 wt% SnO_2 h-NFs, all the observed diffraction peaks agreed with that reported for anatase TiO_2 (JCPDS no. 21-1272). In the case of films containing 100 wt% SnO_2 h-NFs, all the diffraction peaks could be indexed with the peaks reported for rutile-type SnO_2 (JCPDS no. 41-1445). With increasing SnO_2 h-NF concentration, the intensity of peaks related to SnO_2 increased and that corresponding to TiO_2 decreased.

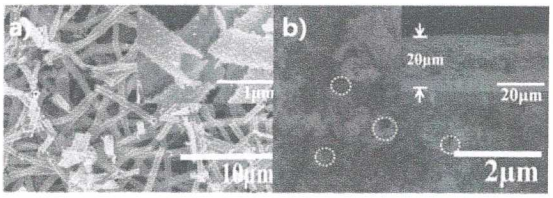

Figure 1. SEM images of (a) SnO_2 h-NFs and (b) the h-NF/TiO_2 NP composite film containing 50 wt% SnO_2 h-NFs. The dotted circles indicate the exposed h-NFs.

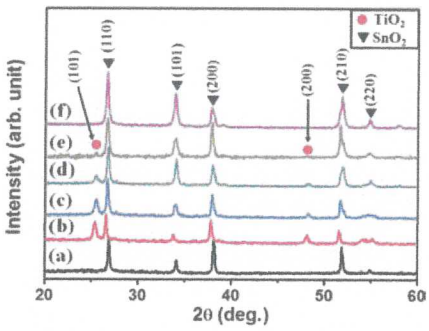

Figure 2. XRD patterns of (a) FTO/glass and (b)–(f) SnO_2 h-NF/TiO_2 NP composite films containing SnO_2 h-NF concentrations of 0, 25, 50, 75, and 100 wt%, respectively.

The characteristic J–V curves of the DSSCs fabricated with h-NF/NP composites containing different concentrations of SnO_2 h-NFs are shown in Figure 3 and the corresponding variation in the various parameters are summarized in Figure 3(b) and Table I. In the case of cells fabricated with samples with 0 wt% SnO_2 h-NFs i.e., those composed of only TiO_2 NPs, the open circuit voltage (V_{OC}), the short circuit current density (J_{SC}), and conversion efficiency (η) were 0.65 V, 6.16 mA/cm^2, and 2.85%, respectively. In the case of DSSCs fabricated with 100 wt% SnO_2 h-NF samples, V_{OC}, J_{SC}, and η were 0.61 V, 4.61 mA/cm^2, and 1.49%, respectively. Hence, the DSSCs employing 100 wt% SnO_2 h-NF films as photoanode showed lower performance than the TiO_2 NP-based systems. This may be due to the lower specific surface area and presence of more vacant spaces in SnO_2 h-NF photoanodes than in the case of electrodes composed of TiO_2 NPs, although SnO_2 h-NFs may be expected to show higher charge transportation rates. Therefore, employing films of solely the h-NFs, which exhibit lower amounts of dye absorption than NPs results in decreased J_{SC} and η. In the case of DSSCs with composite electrodes containing 25 and 75 wt% SnO_2 h-NFs, the J_{SC}, and η were 6.14 mA/cm^2, 2.66% and 5.32 mA/cm^2, 2.45%, respectively. When the concentration of the SnO_2 h-NFs was 50 wt%, the J_{SC} and η were 9.57 mA/cm^2 and 3.43%. The values subsequently declined due to the lower specific surface area when the concentration of SnO_2 h-NFs was increased above 50 wt%.

On an overall, DSSCs with the photoanode containing 50 wt% SnO_2 h-NFs, showed the best performance in terms of J_{SC} and η.

This may have been due to the optimal combination of light scattering and fast electron transport rate in SnO_2 h-NFs and the high specific surface area of TiO_2 NPs. Hence, from these results, it may be inferred that the performance of the DSSCs can be enhanced with an appropriate concentration of SnO_2 h-NFs and TiO_2 NPs.

To investigate the difference in the interfacial characteristics of these photoanodes, we measured the EIS spectra

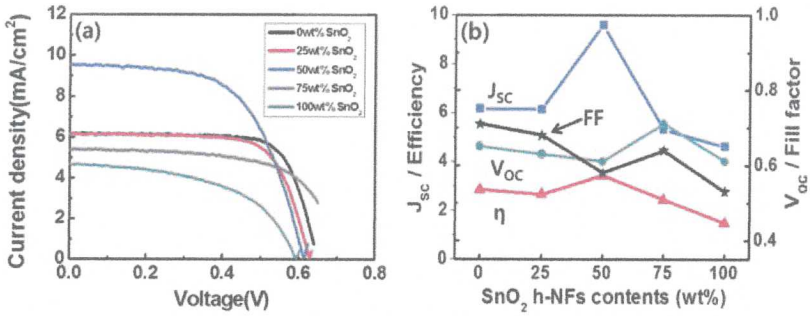

Figure 3. (a) J–V curves and (b) a summary of parameters of DSSCs employing SnO_2 h-NF/TiO_2 NP composite photoanodes as a function of the concentrations of SnO_2 h-NFs.

of the DSSCs as a function of the SnO_2 h-NF concentrations in the composite photoanodes, as shown in Figure 4. In the Nyquist plots shown in Figure 4, the first, second, and third semicircular curves have been derived from the sheet resistance of FTO/glass, the sum of the interfacial resistance of TiO_2/FTO and Pt/electrolyte, and the resistance at the dye-absorbed composite/electrolyte interface, respectively. The largest semicircular curve is attributed to the photo-injected electrons and represents the charge recombination resistance.[8] The diameter of these semicircles for the DSSCs fabricated with composite photoanodes containing 50 wt% SnO_2 h-NFs were much smaller than that of the others, indicating faster charge transfer in the photoanode and interfacial regions. The electron lifetime (τ_r) in the oxide film was evaluated according to $\tau_r = 1/2\pi f_{max}$, where f_{max} is the maximum peak frequency.

As shown in the inset of Figure 4, the τ_r values calculated for DSSCs fabricated with composite photoanodes containing 25, 50, 75, and 100 wt% SnO_2 h-NFs were 2.52, 7.96, 5.93, and 6.34 ms. These values were much larger than the τ_r values shown by DSSCs containing photoanode with 0 wt% SnO_2 h-NFs (of 1.66 ms). Longer τ_r values indicates less charge recombination and high electron transport ratios.[9]

In the DSSCs, the composite film electrodes were designed based on band-edge engineering. The conduction band of SnO_2 is 0.4 eV higher than that of TiO_2. In addition, the electron mobility in SnO_2 is about 100 times higher than that in TiO_2.[8] Thus, the electrons injected into TiO_2 from the excited dye can be expected to be efficiently injected into the SnO_2, and their transfer into the electrode is facilitated. Figure 5 shows the mechanism of electron transport in SnO_2 h-NF/TiO_2 NP composite films. In the case of films with 0 wt% SnO_2 h-NFs, the TiO_2 NPs can provide a zigzag pathway for electron transfer. However the most direct and effective electron transport is possible in the case of SnO_2 h-NFs. Therefore, the crosslinked SnO_2 h-NFs and TiO_2 NPs in the composites can allow for excellent transport of electrons. The maximum η achieved with DSSCs fabricated using composite photoanodes containing 50 wt% SnO_2 h-NFs when compared to films with other SnO_2 h-NF concentrations can be attributed to the optimized conditions of high specific surface area and lower resistance achieved.

Table I. Summary of the performances of DSSCs according to the SnO_2 h-NF concentration in the composite photoanodes.

SnO_2 h-NFs contents (wt%)	V_{OC} (V)	J_{sc} (mA/cm^2)	FF (%)	η (%)
0	0.65	6.16	71	2.85
25	0.63	6.14	68	2.66
50	0.61	9.57	58	3.43
75	0.71	5.32	64	2.45
100	0.61	4.61	53	1.49

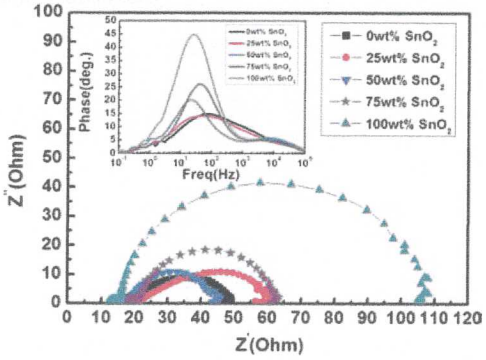

Figure 4. EIS spectra of DSSCs fabricated with SnO_2 h-NF/TiO_2 NP composite phtotoanodes with SnO_2 h-NF concentrations of 0, 25, 50, 75, and 100 wt%. The inset shows the Bode-phase plot of these DSSCs.

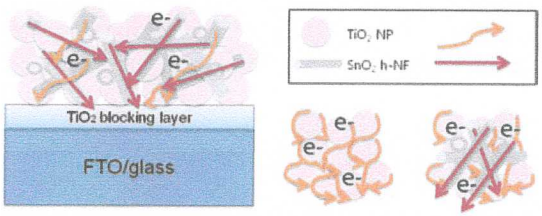

Figure 5. Schematic depicting the electron transport mechanism in DSSCs fabricated with SnO_2 h-NF/TiO_2 NP composite photoanode.

4. CONCLUSIONS

We fabricated composite photoanodes containing SnO_2 *h*-NFs and TiO_2 NPs and investigated the effect of SnO_2 *h*-NF concentrations in the composite on the performance of DSSCs employing these composite photoanodes. The SnO_2 *h*-NFs were uniformly distributed in the composite films. The best η of about 3.43% was measured for DSSCs with composite photoanodes containing 50 wt% SnO_2 *h*-NFs in comparison to DSSCs with TiO_2 NP-based photoanodes ($\eta = 2.85\%$). This result has been attributed to the optimized conditions including photoelectron generation, electron lifetime, shorter electron transfer time, and light scattering achieved by using SnO_2 *h*-NF/TiO_2 NP composite photoanodes.

Acknowledgments: This study was supported by the Korea Research Foundation Grant (KRF-2008-313-D00607) and partially supported by the Converging Research Center Program through the Ministry of Education, Science and Technology (Grant No. 2011K000770).

References and Notes

1. B. O'Regan and M. Gratzel, *Nature,* 353, 737 **(1991)**.
2. P. Wang, S. M. Zakeeruddin, J. E. Moser, M. K. Nazeeruddin, T. Sekiguchi, and M. Gratzel, *Nat. Mater.* 2, 402 **(2003)**.
3. M. Gratzel, *Inorg. Chem.* 44, 6841 **(2005)**.
4. M. Gratzel, *Nature* 414, 338 **(2001)**.
5. K. Ahn, H. U. Lee, S. Y. Jeong, J. P. Kim, J. S. Jin, H. S. Ahn, H. S. Kim, and C. R. Cho, *J. Nanosci. Nanotech.* 12, 6022 **(2012)**.
6. C. Gao, X. Li, B. Lu, L. Chen, Y. Wang, F. Teng, J. Wang, Z. Zhang, X. Pana, and E. Xie, *Nanoscale* 4, 3475 **(2012)**.
7. X. Zhang, V. Thavasi, S. G. Mhaisalkar, and S. Ramakrishna, *Nanoscale* 4, 1707 **(2012)**.
8. C. P. Hsu, K. M. Lee, J. T. W. Huang, C. Y. Lin, C. H. Lee, L. P. Wang, S. Y. Tsai, and K. C. Ho, *Electrochim. Acta* 53, 7514 **(2008)**.
9. H. B. Yang, C. X. Guo, G. H. Guai, Q. L. Song, S. P. Jiang, and C. M. Li, *ACS Appl. Mater. Interfaces* 3, 1940 **(2011)**.

Received: 10 March 2013. Accepted: 10 April 2013.